

**USING A TWO DIMENSIONAL WINDING MODEL TO PREDICT  
WOUND ROLL STRESSES THAT OCCUR DUE TO  
CIRCUMFERENTIAL STEPS IN CORE DIAMETER  
OR TO CROSS-WEB CALIPER VARIATION**

**D. M. Kedl**

3M Company

St. Paul, MN USA

**ABSTRACT**

This paper describes a model for estimating the stresses throughout a wound roll as a function of both radius and width. Width direction stresses are influenced by non-uniform winding tensions created through stacking layers of film with cross-web caliper variation. The model computes the effects of cross-web non-uniformity by dividing the roll into an arbitrary number of cross-web segments, treating each as a separate wound roll with its own winding tension, and tension taper. In order to compute tension, segment diameters are first determined. For this, a special model based upon stacking thick walled cylinders with orthotropic properties is used. Computations of the wound-in pressure and tension are then computed from any existing model that allows the compressive roll modulus to be a function of pressure.

**NOMENCLATURE**

d .....	Roll diameter, in.
$E_r$ .....	Radial compressive modulus, psi
$E_t$ .....	Tangential modulus (Young's modulus), psi
I .....	Moment of inertia, in. <sup>4</sup>
k .....	Beam foundation modulus, psi
q .....	Load density on a beam, lbs./in.
R .....	Roll radius, in.
T .....	Winding Tension, lbs., pli, or psi
V .....	Web velocity, in./sec.
y .....	Beam deflection in radial direction, in.
i .....	Increment subscript
o .....	Initial conditions subscript
$\epsilon$ .....	Strain, in./in.
$\lambda$ .....	Tension taper, dimensionless fraction
$\omega$ .....	Roll angular velocity, rad./sec.

## DEFINITION OF TERMS

Throughout this paper:

**Winding tension** will be defined as the tensile stress in the web freespan at the line where the web is tangent to the wound roll.

**Wound-in tension and pressure** are internal to the roll and computed by the wound roll model.

**Thickness and caliper** are interchangeable terms that refer to the local thickness of the web.

**Down-web** refers to dimension in the direction of the web velocity.

**Cross-web** refers to dimensions in the width direction; normal to the Down-web direction.

**Thin web** refers to calipers of 0.003 inch or less, since this is the limit of the experimental conformation at this time.

**Segment** refers to arbitrary cross-web divisions for the purpose of computing wound-in roll stresses.

**Increment** refers to spacing of the cross-web caliper data used to compute the winding tensions. There are usually several increments in a segment.

## THE ANALYTICAL MODEL

The first part of the model describes how to find the winding tensions at designated wound roll radii. Since winding tension is a function of caliper build-up, it will vary across the web width for each caliper increment. The winding tensions are defined for each increment by the initial tension values at the start of the roll, and the change or taper of tension as the radius builds. Both the winding tension and tension taper are used in the second part of the model to compute the wound in pressure and tension.

The terms *segment and increment* requires further definition. The wound roll width is divided into *increments* which are discrete caliper measurements used to make radius and winding tension computations. *Segments* contain one or more *increment*, and are used to shorten the computation time for wound-in pressures and tensions. Normally, there are 5-10 *increments* for each *segment*. Division of the roll into *segments* is not done until after the winding tensions have been computed for the whole roll, and graphically portrayed on the computer monitor. At that time the *segments* are defined to best portray cross-web differences, and then winding tension averaged for all *increments* included in a *segment*.

### Computing Winding Tensions and Tension Taper

As the diameter builds during winding, we can imagine that different portions of the roll will grow at different rates because of cross-web caliper non-uniformity. Therefore, it is important to determine if we can represent a continuous wide wound roll as a stack of narrow, discrete rolls differing in diameters and radial compressive moduli,  $E_r$ . After all, dividing a continuous web into increments presents no problems where there are no differences in radii and  $E_r$ . Under this condition, we simply define the present wound roll models where cross-web variations are not allowed, and all increments have equal stresses. If the web is stiff, then the outer diameters of each increment will be governed by the radial modulus,  $E_r$ , cross-web

caliper variation, and the bending stiffness of the web in both cross and down-web directions. If the web is not stiff, we can treat each increment independent of its neighbor, using only  $E_r$  and caliper for computations.

To determine the stiffness effects, we represent the outer web wrap on a roll as a beam on an elastic foundation, as shown in Figure 1. The web/beam on a foundation will not be stiff if the deflection of point, A, is independent of forces remote from A, the deflection at A does not induce a local bending moment.

From the beam above, let us consider the deflection in the web at point A. To simplify the math, we will also assume a uniform loading on the web, proportional to the tension per lineal inch divided by the roll radius. Timoshenko has shown that the deflection of a beam on an elastic foundation can be given by the following expression.(2)

$$T = \frac{P}{8EI\beta^3} e^{-\beta x} (\cos \beta x + \sin \beta x) \quad \text{Eqn 1}$$

where

$$\beta = \left( \frac{k}{4EI} \right)^{\frac{1}{4}} \quad \text{Eqn 2}$$

Substituting  $qdx$  for the load,  $P$ , and carrying out the integration for the deflection, we get

$$y = \int_0^b \frac{qdx}{8EI\beta^3} e^{-\beta x} (\cos \beta x + \sin \beta x) + \int_0^c \frac{qdx}{8EI\beta^3} e^{-\beta x} (\cos \beta x + \sin \beta x)$$

$$y = \frac{q}{2k} (2 - e^{-\beta b} \cos \beta b - e^{-\beta c} \cos \beta c) \quad \text{Eqn 3}$$

If  $c$ ,  $b$ , and  $\beta$  are large, then  $e^{-c\beta}$  and  $e^{-b\beta}$  will approach zero, and the deflection,  $y$  will be equal to  $q/k$ . Under normal conditions for a thin web, we can consider  $\beta$  to lie between 12 and 60  $\text{in.}^{-1}$ , and  $b$  and  $c$  between 0.25 and 100 inches. These values give us  $e^{-c\beta}$  and  $e^{-b\beta}$  terms that range from  $e^{-25}$  to  $e^{-10000}$ . All points along the beam under these conditions can be considered free from bending and the loading,  $q$ , is transmitted directly into the wound roll laminate that lies under the on-coming web.

If we set the beam foundation modulus,  $k$ , equal to the radial compressive modulus,  $E_r$ , and convert the pressure caused by the outer wrap to load per unit length,  $q$ , then  $q/E_r$  is the radial deflection under the addition of a single wrap of web. Under normal conditions, the winding tension varies cross-web in response to the caliper variation, creating pressures between the outer wrap and the roll which differ for each increment. If we assume the winding tension is uniform for each increment, and the local compressive modulus equal to  $E_r$ , then the local compression is  $q_i/E_{ri}$ . Therefore, the deflection of the increment depends only upon the pressure created on that increment with the addition of a new wrap of web.

With the above conclusions, winding tension is assumed to depend only upon localized radius differences created by stacking layers of web with non-uniform cross-web thickness. Starting from a uniform core radius, we divide the width into arbitrary increments. The addition of a single web wrap will produce local differences in cross-web radii that are equal to the core radius plus the increment web layer thickness.

If we assume that all parts of the roll are rotating at the same rate, the surface velocity at any position along the web width will be proportional to the increment radius times the roll rotational velocity. The continuity equation below shows the relationship between the incoming web strain, and the variations in strain at any cross-web increment. Normally, the incoming strain is uniform across the width, although this not need be the case.

$$V_o (1 - \epsilon_o) = R\omega (1 - \epsilon_i) \quad \text{Eqn 4}$$

Solving for  $\epsilon_i$

$$\epsilon_i = 1 - \frac{V_o (1 - \epsilon_o)}{R\omega} \quad \text{Eqn 5}$$

to find a first estimate for the winding tension,  $T_i$ , in each increment,

$$T_i = \epsilon_i E_t.$$

As the layers increase, this estimate becomes unacceptably high because real web compresses, decreasing the radii proportional to the increment wound-in pressure, and compressive modulus,  $E_r$ . Corrections for compression in the increment radii are obtained by using a wound roll model written or modified to provide radius values as well as wound-in pressures. From the corrected radii, new winding tensions are computed, and the process may be iterated until the tensions and radii converge to stable values. The winding model used in this paper to compute the roll radius is a based upon stacking orthotropic thick walled cylinders. A brief outline of the derivation of the model is given in the attached **Appendix A** at the end of the paper.

Adding the cross-web calipers for each new layer is necessary to find a first estimate for the increment radii and winding tensions. However, it is not necessary to perform a compressibility correction at each addition. The program runs faster if the total thickness of the wound-on web is divided into 15-50 equal parts, and final winding tension computations made only at these radial locations.

Once the winding tensions are computed for each increment, the roll is divided into segments, before computing tension tapers. In Figure 2 a typical tension-roll radius curve for two segments, where Segment A is at thick caliper location in the web, and B is at a thin location, is shown.

The tension taper is computed from the winding tension radius profiles. For this model, the taper is computed by the expression

$$T = T_o \left[ 1 - \lambda \left( \frac{d - d_o}{d} \right) \right] \quad \text{Eqn 6}$$

As the caliper cross-web profiles change during winding, then the tapers may both increase and decrease. For the high caliper portions, the winding tensions will increase throughout the wound roll, producing a negative taper. The opposite is true for the low caliper "valleys" which produce a positive taper. The winding tension profiles for segments A and B are shown in Figure 3.

### Computing Wound-in Stresses

The second part of the model incorporates the winding tensions into any of several existing models to compute the wound roll stresses. The only requirement in selecting a model is that it will allow  $E_r$  to vary with pressure. The model used in this paper is the TNO (3) model although the Hakiel model (4) is just as good and as fast. Comparisons between the TNO and the Hakiel model have shown that the two compare favorably when the pressure dependent  $E_r$  function for each model is computed from the same experimental data.

## EXPERIMENTAL RESULTS

Comparisons between the model and actual wound in tensions show that the above described method adequately predicts the center wind wound roll as a function of cross-web caliper variation over the web width.

Two types of test were run to evaluate the model. The first type used measured cross-web caliper of a 29 inch wide polyester web as a base for cross-web stress computations. The second type assumed a uniform cross-web caliper on 12 inch wide polyester web that was wound on an aluminum core with a 1.0 inch wide by 0.008 inch thick radial step in the center.

The cross-web caliper measurements for the first test were made with a beta gage. A total of 1,000 cross-web caliper readings were taken every 500 feet along the web length, producing 23 cross-web profiles. In Figure 4, the profile pattern is shown.

The cross-web beta gage profile has a down-web component because the web is not stationary. The slope of the beta gage track over the web surface is the ratio of the down-web speed of the film to cross-web speed of the beta gage. There is certainly error in assuming that down-web caliper variation does not influence the cross-web readings. To minimize the influences, the tests were made under special conditions that created cross web caliper variations considerably higher than the down-web. Additional averaging helped minimize noise, and reduced the 1000 cross-web caliper values to 100. These 100 values defined the increments representing a continuous cross-web caliper variation over 29 inch wide web.

The measured cross-web caliper profiles were at discrete down-web stations. However, continuous down-web profile data was required in order to compute the radii of each segment as the roll builds wrap by wrap. A continuous cross-web caliper was computed from the 23 discrete traces by using a weighted average of any two adjacent traces. For example, assume a given wrap added to the winding roll, required a test caliper profile 25% of the distance between measured profiles #3 and #4, in Figure 4. The model would compute a caliper profile by averaging 1.25 of profile #3 with 0.75 of profile #4. If the required profile fell half way between #3 and #4, then the model would have used a straight one-to-one average. This linear method of estimating the actual cross-web caliper profiles for each segment was used to find the first estimate for the local radii.

The curve shown in Figure 5, shows the predicted wound-in pressure as a function of radius compared to FSR<sup>1</sup> data. The FSR data is based upon the cross-web average of all 29 pads for each FSR that was wound into the roll. The pressure profile is relatively flat, indicating that the pressure cross-web averages are equal throughout the roll.

The curve shown in Figure 6, shows the cross-web variations in wound-in pressures. The FSR data is shown as a radial average of all five pads for different FSRs in the same cross-web segments. The curve represents whole roll averages for both FSR and model. As seen, the model clearly follows the measured pressure values. The noise in the computed data may come from several sources. The biggest is the beta gage itself which is normally requires a large amount of data averaging to provide accurate caliper reading in the 0.001-0.002 inch range. The next biggest error is probably from the down-web caliper component. In either case, the error is most pronounced at the low stresses.

The second test made was to evaluate the model for predicting both cross-web and radial changes in pressure for web wound on a core with cross-web non-uniformity. To do this 0.003 inch thick polyester web was wound on a 3.5 inch diameter aluminum core with a 1.0 by 0.008 inch radial step in the center, as shown in Figure 7.

For this test pull tabs were used to measure the actual wound-in pressure. The pull tabs were inserted into the roll as shown in Figure 8 in order that they could be used to measure a change in pressure at a step. The pull tab covering the step had the pressure of the non-step portion of the roll plus the portion under the step. The curve shown in Figure 9, shows the results.

It should be noted that the tension used in the computation is for 1/3 of the actual center wind tension used for creating the roll. In a number of cases of recent tests, center winding models have shown a tendency to yield values any where from 30% to 60% higher than measured data from pull tabs, FSRs or aluminum cores with strain gages on the inside diameter.

## REFERENCES

- (1.) Timoshenko, S., and Goodier, J.N., Theory of Elasticity 3rd ed., McGraw-Hill, New York
- (2.) Timoshenko, S., Strength of Materials, Part II, 3rd ed., D. Van Nostrand Co. Inc, Princeton, New Jersey. pp 1-10
- (3.) Struik, L., "Lecture Notes on Winding Studies Presentation." TNO Rubber Institute, Delft Netherlands
- (4.) Hakiel, Z., "Nonlinear Model for Wound Roll Stress." TAPPI Journal, Vol. 70, No. 5, pp. 113-117, May 1987.

---

<sup>1</sup> See Appendix B for a description and explanation of both FSRs and pull tabs.

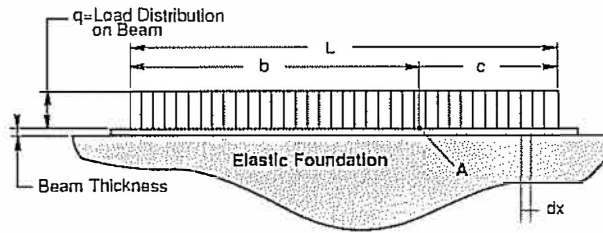


Figure 1

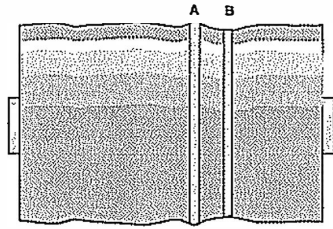


Figure 2

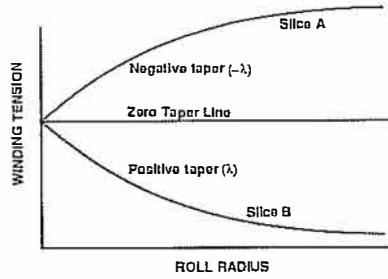


Figure 3

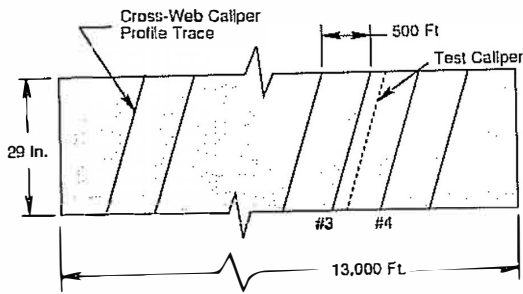


Figure 4

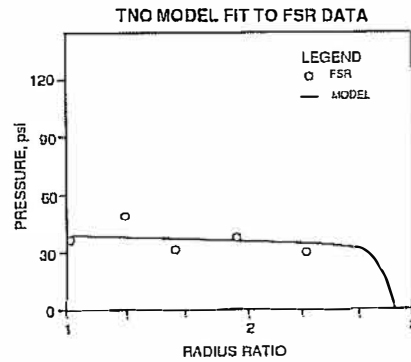


Figure 5

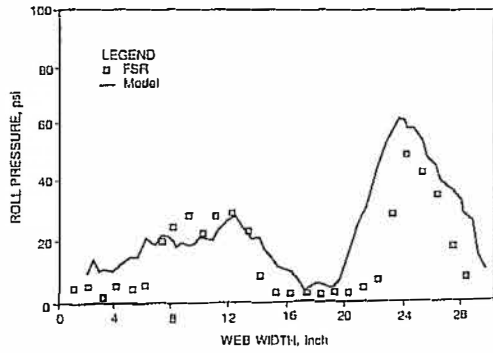


Figure 6

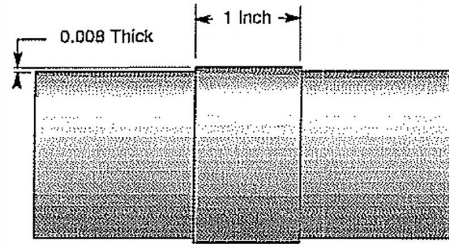


Figure 7

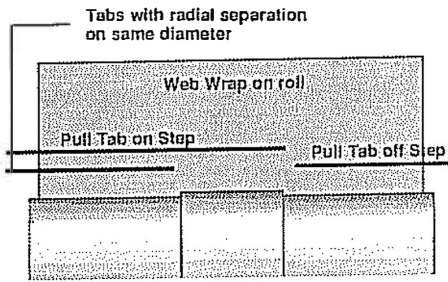


Figure 8

STEP CORE PRESSURES

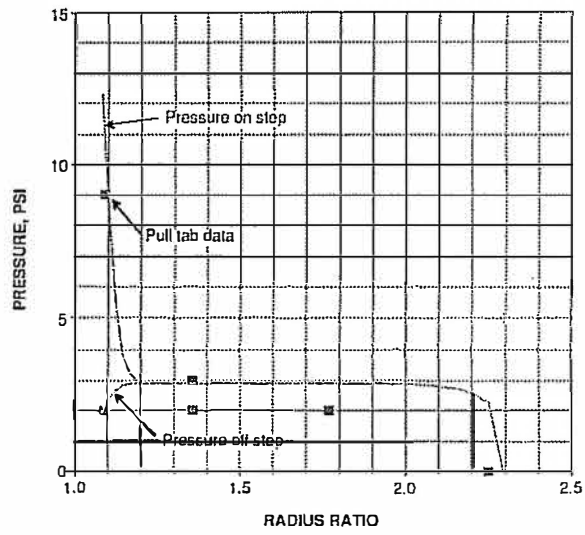


Figure 9



**APPENDIX A  
Nomenclature**

a	.....	Ring inside radius, in.
b	.....	Ring outside radius, in.
E <sub>r</sub>	.....	Radial modulus, psi
E <sub>q</sub>	.....	Tangential modulus, psi
p	.....	Radial pressure on ring, psi
r	.....	Radius, in.
u	.....	Radial deformation, in.
i	.....	Subscript for inside radius
o	.....	Subscript for outside radius
ε <sub>r</sub>	.....	Radial strain, in./in.
ε <sub>q</sub>	.....	Circumferential strain, in./in.
σ <sub>r</sub>	.....	Radial stress, psi
σ <sub>q</sub>	.....	Circumferential stress, psi
ν <sub>q</sub>	.....	Poisson's ratio in tangential direction
ν <sub>r</sub>	.....	Poisson's ratio in radial direction

The following is a copy of portions of the C.A. Copp wound roll model, reproduced with permission. Copp's work was published internal to 3M Company, and did not appear in any of the trade literature or journals. The portion reproduced here shows the derivation of the governing equations, and how they are used to compute wound-in stresses.

The model can be visualized as a series of rings that are interference fit concentrically onto a core of known properties. Each ring mathematically represents a lap of wound-on web material. where the amount of interference between the laps is a function of the wound-in tension, tension profile, and the web material properties. It is this interference that causes the internal stress distribution. Each of the rings has a characteristic radius which represents the stress free state of the rings. If the finished model were disassembled, each of the rings would return to its original stress-free state. The program seeks to solve for this stress-free radius in all of the laps, and from this information, calculates the internal stresses and deformations that would exist in the assembled wound roll.

The rings can be represented by equations for static equilibrium in a cylindrical body. A very thorough derivation can be found from Timoshenko (1), which shows the equations of equilibrium in cylindrical coordinates. In our assumptions, we assume that shear forces are small and that axial symmetric conditions prevail with no effects in the tangential direction and no body forces. With these conditions, the equilibrium equations reduce to

$$\frac{d\sigma_r}{dr} + \nu_\theta \frac{\sigma_r - \sigma_\theta}{r} = 0 \quad \text{Eqn 7}$$

Using this equation, we can solve for pressure and deflections, and from there solve for the tensions.

The roll will also be subject to the constitutive and kinematic equations, which describe the relationships between strain and deformation as shown.

$$\epsilon_r = \left( \frac{\sigma_r}{E_r} - \nu_\theta \frac{\sigma_\theta}{E_\theta} \right) \quad \text{Eqn 8a}$$

$$\epsilon_\theta = \left( \frac{\sigma_\theta}{E_\theta} - \nu_r \frac{\sigma_r}{E_r} \right) \quad \text{Eqn 8b}$$

Combining the expressions for tangential strain yields a useful equation, which describes the radial deformation at radius,  $r$ , due to the tangential and radial stress.

$$\mu = \left( \frac{\sigma_\theta}{\sigma_r} - \nu_r \frac{\sigma_r}{\sigma_\theta} \right) \quad \text{Eqn 9}$$

Since there is a relationship between the radial and tangential stresses, we know that the deformation in a thick cylinder can be fully defined by the radius and the pressure at that radius.

For rotational symmetry, Timoshenko derives the following expressions for a cylinder with a hole at the center.

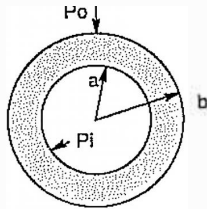
$$\sigma_r = A + \frac{B}{r^2} \quad \text{Eqn 10a}$$

$$\sigma_\theta = A - \frac{B}{r^2} \quad \text{Eqn 10b}$$

Using the notation in the figure shown below, we can find an expression for A and B using the boundary condition:

At  $r=a$ ,  $\sigma_r = -p_i$

At  $r=b$ ,  $\sigma_r = p_o$



Substituting for  $\sigma_r$  in **Eqn 10a**

$$\text{at } r = a \quad -P_i = A + \frac{B}{a^2} \quad \text{Eqn 11a}$$

$$\text{at } r = b \quad -P_o = A - \frac{B}{b^2} \quad \text{Eqn 11b}$$

Solving for A and B simultaneously, and substituting into **Eqn 10a** and **Eqn 10b**,

$$\sigma_\theta = \frac{P_i a^2 - P_o a^2}{b^2 - a^2} + \frac{a^2 b^2 (P_o - P_i)}{r^2 (b^2 - a^2)} \quad \text{Eqn 12a}$$

$$\sigma_r = \frac{P_i a^2 - P_o a^2}{b^2 - a^2} - \frac{a^2 b^2 (P_o - P_i)}{r^2 (b^2 - a^2)} \quad \text{Eqn 12b}$$

The above equations describe the radial and tangential stresses in a thick, hollow cylinder as a function of radius,  $r$ , where  $a < r < b$ . Our interest is where  $r=a$

because this surface will represent the interface between mating rings, or laps of wound-on web. Substituting a and b for r in equations Eqn 12a and Eqn 12b, gives:  
At  $r=a$ ,  $\sigma_r = -p_i$

$$\sigma_{\theta} = P_i \left( \frac{b^2 + a^2}{b^2 - a^2} \right) - P_o \left( \frac{2b^2}{b^2 - a^2} \right) \quad \text{Eqn 13a}$$

At  $r=b$ ,  $\sigma_r = p_o$

$$\sigma_{\theta} = P_i \left( \frac{2a^2}{b^2 - a^2} \right) - P_o \left( \frac{b^2 + a^2}{b^2 - a^2} \right) \quad \text{Eqn 13b}$$

Substituting these into **Eqn 9**, gives:  
at  $r = a$

$$u_a = \frac{a}{E_{\theta}} \left[ P(i) \left( \frac{b^2 + a^2}{b^2 - a^2} + \nu_r \frac{E_{\theta}}{E_r} \right) - P_o \left( \frac{2a^2}{b^2 - a^2} \right) \right] \quad \text{Eqn 14a}$$

at  $r = b$

$$u_b = \frac{b}{E_{\theta}} \left[ P(i) \left( \frac{2a^2}{b^2 - a^2} \right) - P_o \left( \frac{b^2 + a^2}{b^2 - a^2} + \nu_r \frac{E_{\theta}}{E_r} \right) \right] \quad \text{Eqn 14b}$$

**Eqn 14a** and **Eqn 14b** describe the deformation of a thick cylinder due to internal and external pressures. The values a and b are the original, stress-free radii and will be designated  $a_o$  and  $b_o$  From here on. These radii are constant, and as much a property of the ring as  $E_t$  and  $E_r$ . The only unknowns are  $p_i$  and  $p_o$ .

Let us define

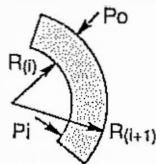
$$a_1 = a_o + u_a \quad b_1 = b_o + u_b$$

Where  $a_1$  and  $b_1$  are the final inside and outside radii, respectively.

$$a_1 = a_o + \frac{a_o}{E_{\theta}} \left[ P(i) \left( \frac{b_o^2 + a_o^2}{b_o^2 - a_o^2} + \nu_r \frac{E_{\theta}}{E_r} \right) - P_o \left( \frac{2a_o^2}{b_o^2 - a_o^2} \right) \right] \quad \text{Eqn 15a}$$

$$b_1 = b_o + \frac{b_o}{E_{\theta}} \left[ P(i) \left( \frac{2a_o^2}{b_o^2 - a_o^2} \right) - P_o \left( \frac{b_o^2 + a_o^2}{b_o^2 - a_o^2} + \nu_r \frac{E_{\theta}}{E_r} \right) \right] \quad \text{Eqn 15b}$$

We now know the radii of the ring at any time as a function of  $p_i$ ,  $p_o$ , and the original inside radius,  $a_o$ . The outside radius,  $b_o$ , is not an independent variable since  $b_o = a_o + \text{web thickness}$ . Therefore, the ring is defined.



Once a series of rings are stacked together, their deformed radii and interface pressures are dependent upon their neighbors. The sketch at left shows two interfaces of an arbitrary ring inside the

roll. There are two variables of interest at each interface, pressure and radius. If any two of these quantities are known, the two equations for an inner ring,  $i$ , will give the other two. Eqn 15a and Eqn 15b can be used to find  $R(i)$  and  $P(i)$  as follows:

$$P(i) = \left( \frac{b_o^2 - a_o^2}{2a_o^2} \right) \left[ \frac{E_\theta}{b_o} (R(i+1) - b_o) + P(i+1) \left( \frac{b_o^2 + a_o^2}{b_o^2 - a_o^2} - \frac{E_\theta}{E_r} \nu_r \right) \right] \text{Eqn 16a}$$

$$R(i) = a_o + \frac{a_o}{E_\theta} \left[ P(i) \left( \frac{b_o^2 + a_o^2}{b_o^2 - a_o^2} - \frac{E_\theta}{E_r} \nu_r \right) - P(i+1) \left( \frac{2b_o^2}{b_o^2 - a_o^2} \right) \right] \text{Eqn 16b}$$

In turn,  $P(i)$  and  $R(i)$  can be used to define  $P(i+1)$  and  $R(i+1)$ , and so on down through the stack of rings to the hub. Eqn 16a and Eqn 16b are used in the computer program.

The core is also a thick walled cylinder with no pressure on the inside surface and will be assumed to be isotropic. The outside pressure is due to the wound-on material, and the radial deformation of the core has to be consistent with that pressure. The core response is the inside boundary condition. Eqn 15b describes the core when

$$\begin{aligned} p_i &= 0 \\ E_q &= E_r \\ R_o &= b_o \\ R_i &= a_o \end{aligned}$$

and we have,

$$R_{\text{core}} = R_o - \frac{R_o}{E_{\text{core}}} \left( \frac{R_o^2 + R_i^2}{R_o^2 - R_i^2} \right) P_o \quad \text{Eqn 17}$$

The pressure exerted by the stack on the hub has to be consistent with the deflection of the hub. If the deflection of the stack differs from the deflection of the hub for the same interface pressure, then the roll has lost its continuity, and the solution for radii and pressures throughout the roll is incorrect. Such being the case, some corrective iteration must take place.

During roll building, laps or rings are laid on one at a time. Because of the radial compressibility, the original radius of the new lap is unknown. We do not know how much the stack will compress under the pressure of the newly added ring. It is required that the ring have a specified tension after all boundary conditions are met, that will be the outer boundary condition of the web tension in pli divided by the roll radius. We also know that for the outside ring  $p_o = 0$ . Applying Eqn 12b for  $r = a$  and  $p_o = 0$

$$\sigma_\theta = P_i \left( \frac{b_o^2 + a_o^2}{b_o^2 - a_o^2} \right) \quad \text{Eqn 18a}$$

or

$$P_i = \sigma_\theta \left( \frac{b_o^2 - a_o^2}{b_o^2 + a_o^2} \right) \quad \text{Eqn 18b}$$

We assume a value for  $a_o$ , and using the specified winding tension,  $\sigma_{wind}$ , a value for  $p_i$  is found. Now from Eqn 15b where  $p_o = 0$  for the outside ring,

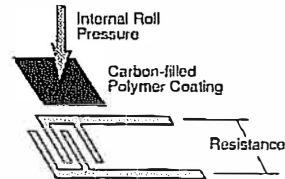
$$a_1 = \sigma_\theta + \frac{a_o}{E_\theta} \left( \frac{b_o^2 + a_o^2}{b_o^2 - a_o^2} + \nu_r \frac{E_\theta}{E_r} \right) P_i \quad \text{Eqn 19}$$

These two values under the new lap are run down through the stack of rings to compute a new radius and pressure for the hub. If the predicted core radius does not agree with the stack radius, then a new value for  $a_o$  is chosen and the computations repeated until the stack radius is not significantly different than the core radius.

## APPENDIX B Descriptions of FSR and Pull Tabs

### FSR Description

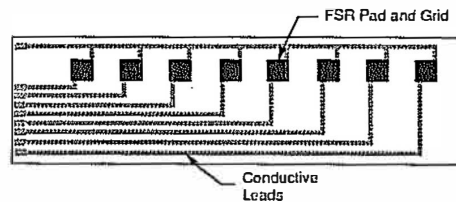
FSR stands for Force Sensing Resistor, and is the invention of InterLink Electronics of Santa Barbara, California. The sketch at right shows the FSR construction.



The device consists of two parts. One is a conductive ink, screen printed on a high modulus backing to form two interleaving, but non-contacting grids. The other is a screen printed pad of ink containing carbon. When the pad is pressed into the conductive grids, there is a change in electrical resistance across the two grid connector points.

The FSR was designed as a membrane switch to provide off/on control, rather than as a pressure transducer. The device does provide a non-linear pressure-resistance relationship, though it is not recommended or sold for that purpose. Only through a great deal of effort and care in calibration can the FSR can be used as a thin pressure transducer. The obvious advantages of inserting them directly into the winding roll for direct pressure measurement helps compensate for the handling difficulties.

The FSR used in for experimental evaluation was specifically designed by 3M Company to measure both cross-web and radial pressures. Two configurations were made, one for 7 pads, and the other for 30. A sketch of the basic layout is shown below.



The thickness of the FSR is 0.004 inches. The FSR may be re-used many times, but must be calibrated frequently to account for effects of moisture, and changes in the pad surfaces.

### **Pull Tab Description**

The pull tab is not a new device, and is described here only to record the construction of the specific device used for this paper. A sketch of the device is shown below.

The advantage of the brass sleeve is to reduce the need for calibrating the tabs for every material used. The device can be reused several times.

